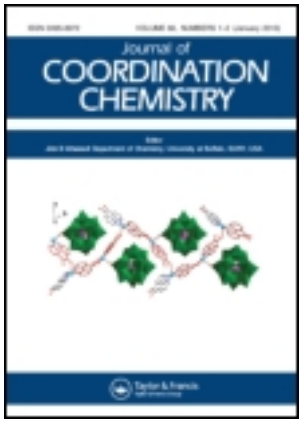

Journal of Coordination Chemistry
Publication details, including instructions for authors and subscription information:
http://www.tandfonline.com/loi/gcoo20

Two coordination polymers based on semicarbazone Schiff base and azide: synthesis, crystal structure, electrochemistry, magnetic properties and biological activity

Behrouz Shaabani [a], Ali Akbar Khandar [a], Michal Dusek [b], Michaela Pojarova [b], Farzaneh Mahmoudi [b], Alexander Feher [c] & Marcela Kajňaková [c]

[a] Faculty of Science, Department of Inorganic Chemistry, Tabriz University, Tabriz, Iran

[b] Institute of Physics ASCR, Praha, Czech Republic

[c] Faculty of Science, Centre of Low Temperature Physics, P. J. Safarik University in Kosice, Park Angelinum, Slovakia

Accepted author version posted online: 18 Jan 2013.Published online: 13 Mar 2013.

To cite this article: Behrouz Shaabani, Ali Akbar Khandar, Michal Dusek, Michaela Pojarova, Farzaneh Mahmoudi, Alexander Feher & Marcela Kajňaková (2013) Two coordination polymers based on semicarbazone Schiff base and azide: synthesis, crystal structure, electrochemistry, magnetic properties and biological activity, Journal of Coordination Chemistry, 66:5, 748-762, DOI: 10.1080/00958972.2013.764413

To link to this article: http://dx.doi.org/10.1080/00958972.2013.764413

Journal of Coordination Chemistry
Vol. 66, No. 5, 10 March 2013, 748–762

Two coordination polymers based on semicarbazone Schiff base and azide: synthesis, crystal structure, electrochemistry, magnetic properties and biological activity

BEHROUZ SHAABANI*†, ALI AKBAR KHANDAR†, MICHAL DUSEK‡, MICHAELA POJAROVA‡, FARZANEH MAHMOUDI†, ALEXANDER FEHER§ and MARCELA KAJŇAKOVÁ§

†Faculty of Science, Department of Inorganic Chemistry, Tabriz University, Tabriz, Iran
‡Institute of Physics ASCR, Praha, Czech Republic
§Faculty of Science, Centre of Low Temperature Physics, P. J. Safarik University in Kosice, Park Angelinum, Slovakia

(*Received 27 February 2012; in final form 23 October 2012*)

$[Mn(L)(\mu_{1,1}\text{–}N_3)_2]_{2n}[Mn(H_2O)_2(\mu_{1,1}\text{–}N_3)_2]_n$ (**1**) and $[Cd(HL)(\mu_{1,1}\text{–}N_3)_2]_n$ (**2**) have been synthesized from HL (HL: pyridine-2-carbaldehyde semicarbazone) and azide ligands, characterized by FT-IR, UV–vis spectroscopy and X-ray crystallography. Single crystal X-ray diffraction revealed that **1** is a coordination polymer consisting of two infinite 1-D chains: chain A with $[Mn(L)(\mu_{1,1}\text{–}N_3)_2]_{2n}$ and chain B with $[Mn(H_2O)_2(\mu_{1,1}\text{–}N_3)_2]_n$. In both chains, Mn centers are connected via two double end-on (EO) azide bridges. **2** is a coordination polymer consisting of a 1-D infinite chain, where Cd centers are connected via two double EO azide bridges. The electrochemistry of HL, **1** and **2** were studied by cyclic voltammetry. Magnetic susceptibility measurements indicate bulk ferromagnetic coupling for **1** below 5 K. Antimicrobial activities of both compounds **1** and **2** were greater than HL, with the strongest effect for **2** consistent with its larger radius and electronegativity of Cd(II) ions.

Keywords: Semicarbazone ligand; Azide ligand; Coordination polymer; X-ray structure; Antimicrobial activity

1. Introduction

Transition metal coordination polymers with Schiff base ligands draw attention because of interesting structural features and applications in catalysis, magnetism, light emission and biological modeling [1–19]. The Schiff base ligands are obtained through straightforward synthetic pathways [6,19–21]. Semicarbazones and thiosemicarbazones can coordinate to metal centers in neutral or deprotonated form, yielding complexes with applications as anticancer, antibacterial, antifungal, or antivirus agents [13,22–26]. Pseudohalides (N_3^-, NCS^-, NCO^-) are versatile ligands [27–29]; azide bridging ligands can link two or more metal ions, $\mu\text{-}_{1,1}$ (*end-on*, EO) or $\mu\text{-}_{1,3}$ (*end-to-end*, EE). The bridging modes strongly influence magnetic interactions between adjacent metal ions,

*Corresponding author. Email: shaabani@tabrizu.ac.ir

Journal of Coordination Chemistry
ISSN 0095-8972 print/ISSN 1029-0389 online
http://dx.doi.org/10.1080/00958972.2013.764413

ranging from antiferromagnetic to ferromagnetic coupling [30–34]. Complexes with symmetric EO and symmetric EE bridging modes have strong ferromagnetic and antiferromagnetic interactions, respectively, but magnetic properties of asymmetric EO complexes range from weak ferromagnetic to slightly antiferromagnetic, and magnetic properties of asymmetric EE complexes range from slightly ferromagnetic to strongly antiferromagnetic [33–35]. A goal of our recent research has been the search of new compounds of semicarbazone and azide ligands. We had synthesized semicarbazones of pyridine 2-carbaldehyde and azide with Mn(II) and Cd(II). We herein report characterization and X-ray crystal structure analysis of Mn(II) and Cd(II) coordination polymers and also the electrochemistry behavior and the antimicrobial activities. Magnetic behavior was measured only for **1**.

2. Experimental

2.1. *Materials and methods*

All chemicals and solvents were reagent grade and used without purification except HL, which was prepared with the reflux method according to a literature procedure [26]. NMR spectra were recorded on a Bruker Avance 400 in DMSO with $SiMe_4$ as internal standard at room temperature. Microanalyses were carried out using a Heraeus CHN–O–Rapid analyzer. Melting points were measured on an Electrothermal 9100 apparatus and are uncorrected. IR spectra were recorded on a FT-IR Spectrometer Bruker Tensor 27 from 4000 to 400 cm^{-1} using KBr pellets. Electronic spectra were recorded on a Shimadzu, UV-1650 PC spectrophotometer from DMSO solution. Cyclic voltammetric measurements were performed using an AMEL Instruments Model 2053 as potentiostat connected with a function generator (AMEL Model 568). In all electrochemical studies, a three-electrode system was used consisting of glassy carbon as the working electrode, a platinum wire auxillary electrode, and an Ag/AgCl as the reference electrode. Electrochemical experiments were carried out under nitrogen at room temperature using 10^{-3} M solution of complexes in DMSO containing 0.1 M lithium perchlorate as the supporting electrolyte. Electrochemistry of HL and its metal compounds were studied by cyclic voltammetry with scan rate of 0.010 Vs^{-1} in DMSO containing 0.1 M lithium perchlorate supporting electrolyte. Ferrocene (Fc) was used as the internal standard and all redox potentials referenced to the Fc+/0 couple.

2.2. *Synthesis*

2.2.1. Synthesis of HL. Schiff base HL [HL: pyridine-2-carbaldehyde semicarbazone] was prepared by condensation of pyridine-2-carbaldehyde with semicarbazide by reflux method [36–39]. Yield: 1.20 g (5 mmol, 80%) [m.p. 190 °C]. Anal. Calcd for $C_7H_8N_4O$: C, 45.7; H, 4.5; N, 30.1. Found: C, 45.9; H, 4.3; N, 30.3. Characteristic IR absorptions (cm^{-1}): 3412 m, ν(NH2); 3162 m, ν(NH); 1613 s, ν(C=N); 1091 s, ν(NN); 1685 s, ν(C=O). ^{1}H NMR: δ (ppm) = 11.28 (s, 1H, NH); 8.75 (d, 1H, C(1)H); 7.85 (t, 1H, C(2)H); 8.55 (t, 1H, C(3) H); 8.29 (d, 1H, C(4)H); 8.03 (s, 1H, C(6)H); 7.95 (s, 2H, NH2).

2.2.2. Synthesis of the complexes. *Caution!* Metal azide complexes are potentially explosive. Only a small amount of material should be prepared and handled with caution.

2.2.2.1. *[Mn(L)($\mu_{1,1}$–N_3)$_2$]$_{2n}$*[Mn(H_2O)$_2$($\mu_{1,1}$–N_3)$_2$]$_n$ (**1**). Synthesis as crystalline material was performed by the branched tube method [40–44]. In this method, 0.2 mmol HL, 0.4 mmol $MnCl_2 \cdot 4H_2O$ and 1.5 mmol NaN_3 in ethanol were used. After two days, yellow crystals (decomposition at 190 °C) formed, were isolated by filtration, washed with acetone and diethyl ether and dried in air. Yield: 0.12 g, 60%. Anal. Calcd for $C_{14}H_{18}Mn_3N_{26}O_4$: C, 21.67; H, 2.32; N, 46.95. Found: C, 21.77; H, 2.44; N, 46.95. Characteristic IR absorptions (cm^{-1}): 3415 m, ν(NH_2); 1611 s, ν(C=N); 1165 s, ν(N–N); 1651 s, ν(C=O); 2058, 2090 s, ν(N_3^-).

2.2.2.2. *[Cd(HL)($\mu_{1,1}$–N_3)$_2$]$_n$* (**2**). Using similar method as for **1**, 0.2 mmol HL, 0.75 mmol $Cd(OAc)_2 \cdot 2H_2O$ and 1.5 mmol NaN_3 in methanol were used. After three days, light yellow crystals (decomposed at 220 °C) formed, were filtered off, washed with acetone and diethyl ether and dried in air. Yield: 0.09 g, 45%. Anal. Calcd for $C_7H_8CdN_{10}O$: C, 23.30; H, 2.20; N, 38.80. Found: C, 23.40; H, 2.3; N, 38.80. Characteristic IR absorptions (cm^{-1}): 3418 m, ν(NH_2); 3184 m, ν(NH); 1608 s, ν(C=N); 1172 s, ν(N–N); 1678 s, ν(C=O); 2057 s, ν(N_3^-). ^{1}H NMR: δ (ppm) = 11.62 (s, 1H, NH); 8.95 (d, 1H, C(1)H); 8.10 (t, 1H, C(2) H); 8.87 (t, 1H, C(3) H); 8.52 (d, 1H, C(4)H); 8.46 (s, 1H, C(6)H); 8.35 (s, 2H, NH_2).

2.3. *Crystal structure determination*

X-ray diffraction data were collected at 120 K with a four-circle diffractometer Gemini of Oxford Diffraction, Ltd. using a sealed X-ray tube with copper anode. The primary beam was collimated by mirrors using the Enhance-Ultra collimator; diffracted beams were detected with the CCD detector Atlas. Standard data collection strategy of Crysalis [45] was used for data collection as well as for data processing. Experimental details are given in tables 2–4.

2.4. *Magnetic measurement*

Susceptibility and magnetization were investigated in a commercial Quantum Design MPMS apparatus. In these measurements, the sample was held in an inert gelcap. Temperature dependence of susceptibility of polycrystalline sample was investigated from 2 to 300 K in applied magnetic fields 10 mT (100 Gauss). The background correction of the signal resulting from the gelcap and a sample holder was defined from independent run with empty gelcap and subtracted from the total signal. Diamagnetic contribution of the material to the susceptibility was estimated using Pascal's constants and subtracted from the total susceptibility.

Table 1. Infrared spectra (cm^{-1}) assignment for HL, **1** and **2**.

Compound	ν_{NH2}	ν_{NH}	$\nu_{C=O}$	$\nu_{C=N}$	$\nu_{N=C}$	ν_{N-N}	ν_{N3}
HL	3412	3162	1685	1613	–	1091	–
1	3415	–	1651	1611	1555	1165	2058, 2090
2	3418	3184	1648	1608	1546	1172	2057

Table 2. Crystal and structure refinement data for **1** and **2**.

	1	**2**
Formula	$2(C_7H_7MnN_{10}O)MnN_6O_2H_4$	$C_7H_8CdN_{10}O$
Formula weight	775.33	360.63
Crystal size (mm)	$0.16 \times 0.04 \times 0.03$ mm	$0.15 \times 0.10 \times 0.02$ mm
Crystal system	Monoclinic	Monoclinic
Space group	*C2/c*	$P2_1/c$
a (Å)	44.6934(16)	18.2423(9)
b (Å)	9.6802(3)	9.7255(4)
c (Å)	6.5293(2)	6.5488(3)
α (°)	90	90
β (°)	91.605(4)	97.243(4)
γ (°)	90	90
Volume (Å^3)	2823.73(16)	1152.59(9)
Z	4	4
$\rho_{calculated}$ (g cm^{-3})	1.824	2.078
μ (mm^{-1})	11.44	15.33
θ Range (°)	4.0–67.1	4.9–67.2
Reflections collected	10,710	10,796
Independent reflections	2502	2042
Final R indices [$I > 2\sigma(I)$]	0.1386; 0.3640	0.0388; 0.0941
Final R indices (all data)	0.1501; 0.3711	0.0518; 0.1000
Largest diff. peak and hole (eÅ^{-3})	4.594; −1.204	0.670; −1.042

Table 3. Selected bond lengths (Å) and angles (°) for **1** and **2**.

Part A of compound **1**		Part B of compound **1**		Compound **2**	
Mn1–O1	2.413(10)	Mn2–O2	2.177(10)	Cd1–N3	2.464(5)
Mn1–N9	2.343(12)	Mn2–N11	2.204(13)	Cd1–N4	2.541(4)
Mn1–N10	2.421(12)	Mn2–N11c	2.265(13)	Cd1–O1	2.490(4)
Mn1–N1	2.284(13)	N11–N12	1.194(19)	Cd1–N5	2.443(5)
Mn1–N1b	2.228 (13)	N12–N13	1.161(19)	Cd1–N5a	2.320(5)
Mn1–N4	2.295(12)	O2–Mn2–O2c	176.9(6)	Cd1–N8	2.364(4)
Mn1–N4b	2.288(12)	O2–Mn2–N11f	90.6(5)	Cd1–N8b	2.311(5)
N1–N2	1.227(18)	O2–Mn2–N11	87.3(5)	N5–N6	1.200(7)
N2–N3	1.136(19)	O2–Mn2–N11d	92.0(5)	N6–N7	1.166(7)
N4–N5	1.208(17)	N11–Mn2–N11c	176.7(6)	N8–N9	1.193(6)
N5–N6	1.150(18)	N11–Mn2–N11f	96.1(7)	N9–N10	1.156(7)
		N5–Cd1–O1	146.02(14)		
N1–Mn1–N4	75.2(4)		N5–Cd1–N5a	109.19(16)	
N1–Mn1–O1	94.1(4)		N5–Cd1–N8	81.99(16)	
N1–Mn1–N9	85.4(4)		N5–Cd1–N8b	74.35(16)	
N1–Mn1–N4b	171.8(5)		N5–Cd1–N3	138.26(15)	
N1–Mn1–N1b	113.0(5)		N5–Cd1–N4	79.42(15)	
N1–Mn1–N10	81.9(4)		N8–Cd1–N3	139.69(15)	
N4–Mn1–O1	76.8(4)		N8–Cd1–N4	145.56(16)	
N4–Mn1–N9	136.4(4)		N8–Cd1–O1	81.66(14)	
N4–Mn1–N4b	110.8(5)		N8–Cd1–N8b	102.19(15)	
N4–Mn1–N1b	82.4(4)		N3–Cd1–N4	65.21(14)	
N4–Mn1–N10	143.5(4)		N3–Cd1–O1	63.99(12)	
N4–Mn1–N1	74.0(4)		N3–Cd1–N5a	88.80(16)	
O1–Mn1–N1b	140.1(4)		N3–Cd1–N8b	90.31(15)	
O1–Mn1–N4b	82.1(4)		N4–Cd1–O1	129.16(13)	
O1–Mn1–N9	66.0(4)		N4–Cd1–N5a	79.42(15)	
O1–Mn1–N10	133.7(4)		N4–Cd1–N8b	100.35(16)	
			N5a–Cd1–N8b	175.38(15)	

Table 4. Selected hydrogen bonding parameters in **1** and **2**.

D – H···A	D – H (Å)	H···A (Å)	D···A (Å)	D – H···A (°).
Compound **1**				
N7 – H2N7···N13^{i}	1.14	1.93	3.059(19)	170
N7 – H1N7···N11^{ii}	1.13	2.06	3.080(19)	149
N7 – H1N7···N12^{ii}	1.13	2.50	3.325(19)	129
C4 – H4···N3^{iii}	0.93	2.45	3.33(2)	157
Compound **2**				
N1 – H1N1···O1^{v}	0.71	2.35	2.864(6)	130
N2 – H1N2···N10^{vi}	1.05	1.94	2.877(6)	146

Symmetry codes: (i) x, $-y+1$, $z+1/2$; (ii) x, $y+1$, z; (iii)$-x+1$, $-y+1$, $-z+1$; (iv) x, $-y+2$, $z+1/2$; (v)$-x+1$, $-y+2$, $-z$; (vi) x, $y+1$, z.

2.5. *Antimicrobial activity*

The free ligand and its metal complexes were screened for antimicrobial activities against bacteria (*Bacillus subtilis*, *Staphylococcus aureus*, *Escherichia coli*, *Erwinia carotovora*) and fungi (*Candida kefyr*, *Candida krusei*, *Aspergillus niger*) by the disk diffusion method as Gram negative, Gram positive and fungal organisms, respectively. The culture media (Miller hinton agar for bacteria, Sabouraud dextrose agar for fungi) was poured into sterile plates and microorganisms were introduced on the surface of agar plates individually. Blank sterile disks of 6.4 mm diameter were soaked in a known concentration of the test compounds. Then the soaked disks were implanted on the surface of the plates. A blank disk was soaked in DMSO and implanted as negative control on each plate along with the standard drugs. The plates were incubated at 37 °C (24 h) and 27 °C (48 h) for bacterial and fungal strains, respectively. The MIC for each tested substance was determined by macroscopic observation of microbial growth as the lowest concentration of the tested substance where microbial growth was clearly inhibited.

3. Results and discussion

Both reported compounds include chains of metal bridged by double EO azide. In **1**, the deprotonated semicarbazone chelates in the enolate form, as proven by IR spectral data, while in **2**, the ligand is in the keto form. In **1**, unfortunately, due to the bad quality of crystal data, the imine hydrogen and hydrogens belonging to water could not be found from the maps of residual electron density, and therefore, enolate form of HL indicated in IR spectra could not be confirmed by X-ray study. For **2**, X-ray data clearly confirm the presence of imine hydrogen and coordination of HL in the keto form. Most semicarbazone ligands reveal keto-enol tautomerism in coordination to metal [46].

3.1. *Infrared spectra*

IR spectra of **1** and **2** were compared with that of free ligand. A medium band at 3162 cm^{-1}, present for the free ligand due to ν_{N-H}, disappears in spectra of **1**, providing strong evidence for ligand coordination to Mn in the enolate form. In **2**, ν_{N-H} is present, since this compound has HL in the keto form [19,36,46]. The strong band at 3412 cm^{-1} in HL, assigned to ν_{N-H}, shifts to higher energies in **1** and **2**, see table 1. The $\nu_{C=N}$ of

semicarbazone is shifted to lower frequencies in the complexes, indicating coordination via the azomethine nitrogen [14,36,38,39]. Coordination of this nitrogen is supported by a shift in ν_{N-N} to higher frequencies [47]. In spectra of all the compounds bands corresponding to newly formed N=C due to enolization of the ligand are present at 1550 cm^{-1}. The strong band at 2000–2100 cm^{-1} indicates the presence of azide in **1** and **2** [2,14,47,48]. **1** exhibits a strong band at 2058 cm^{-1}, with a small shoulder at higher frequency (2090 cm^{-1}), indicating the presence of the two different azide groups, while **2** exhibits a sharp strong band at 2057 cm^{-1} for azide.

3.2. *Electronic spectra*

UV–Vis spectra of HL, **1** and **2** were recorded in DMSO. Electronic spectrum of the ligand shows an absorption at 300 nm attributed to intra-ligand $\pi \rightarrow \pi^*$ transitions of the pyridine ring and azomethine [39]. In the spectrum of **1** and **2**, this band was shifted to 298 and 295 nm, respectively, indicating the nitrogen of imine was involved in coordination [17,39,49]. The other band at 395 and 400 nm for **1** and **2**, respectively, is azide to metal charge transfer [12,27].

3.3. *Crystal structures*

3.3.1. $[Mn(L)(\mu_{1,1}\text{–}N_3)_2]_{2n}]Mn(H_2O)_2(\mu_{1,1}\text{–}N_3)_2]_n$ (1). The ORTEP diagram with atom labeling scheme of **1** is depicted in figure 1 and the crystal data and structure refinement of **1** are summarized in table 2. The compound crystallizes in the monoclinic system, with space group *C2/c*. Single X-ray crystal analysis reveals **1** consists of two infinite 1-D chains (figure 2) of Mn bridged by double EO azides (see figure 3). In chain A with $[Mn(L)(\mu_{1,1}\text{–}N_3)_2]_{2n}$, Mn(III) shows coordination number seven with a distorted pentagonal–bipyramidal geometry [49]. The equatorial plane of the pentagon is formed by two nitrogens of azide (N1b and N4) and two nitrogens and one oxygen of HL (N9, N10 and O1). Axial coordination sites are occupied by two nitrogens of another two azides (N1 and N4b) with N1–Mn1–N4b of 171.8(3)°. By calculating the N1bN10N9O1N4Mn1 plane for the five equatorial atoms and Mn, only Mn and N9 are approximately on this plane with distances about 0.006 and 0.023 Å, respectively, from the plane; N10 is above the plane 0.406 Å and O1 is below 0.399 Å with O1Mn1N10 of 133.71°, also N4 and N1 are above and below about 0.653 and 0.642 Å, respectively, from the plane with N1Mn1N4 of 82.41°. The Mn–N_{azide} distances are 2.226(9)–2.295(8) Å, whereas the Mn–N_{HL} distances are 2.341 (9)–2.420(9) Å. The EO azide bridges show asymmetric N–N distances of 1.227(12)/1.136 (13) Å and 1.207(12)/1.153(13) Å and are quasi-linear [N1–N2–N3, 177.80°; N4–N5–N6, 179.10°]. The four-membered Mn1–N1–Mn1a–N4 rings are planar as usual for double EO bridges. Adjacent Mn1–N1–Mn1a–N4 rings are mutually twisted with dihedral angle 73.14°, close to the dihedral angle found in similar complexes [50]. The closest Mn1…Mn1 distance of 3.618 Å is similar to those found in related compounds: 3.634(1) Å in $[Mn(tptz)(\mu_{1,1}\text{–}N_3)_2]_n$ [tptz: 2,4,6-tris(2-pyridyl)-1,3,5-triazine] [51]; 3.459 Å in $[Mn(bphz)(N_3)_2]_n$ [bphz: 2-benzoylpyridine hydrazone] [50]; 3.459 Å in $[Mn(mipc)(N_3)_2]_n$ [mipc: methyl imidopyrazine carboxylate] [50]; 3.455(6) Å in $[Mn(N_3)_2(bipy)]_n$ [52]; 3.472 Å in $[MnL(N_3)_2]_2 \cdot 2CH_3OH$ [L is a Schiff base ligand which is derived from pyridine-2-carbaldehyde and 2-aminoethyl benzimidazole] [53]. In chain B with $[Mn(H_2O)_2(\mu_{1,1}\text{–}N_3)_2]_n$, the coordination sphere of each Mn(II) contains four nitrogens (N11, N11c, N11d, N11f) from

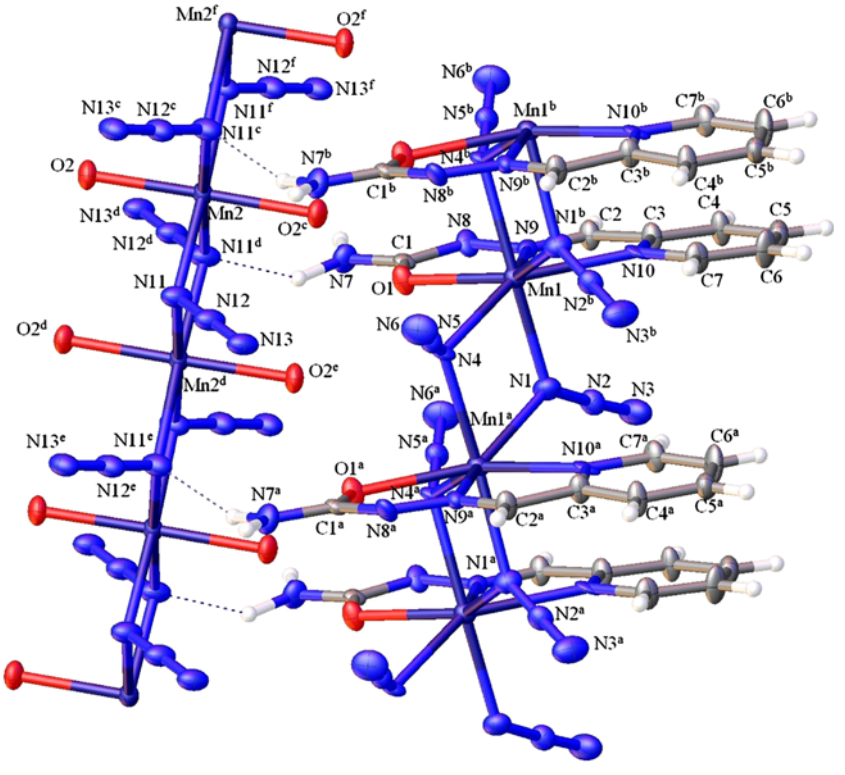

Figure 1. ORTEP diagram of **1** with atom labeling scheme.

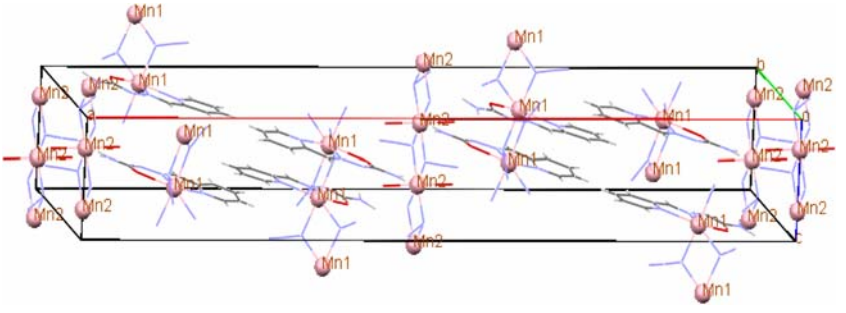

Figure 2. View of the unit cell of **1** in the direction of the crystallographic *b* axis.

bridging azides in the equatorial plane of a distorted octahedron and two oxygens of water (O2 and O2c) in axial sites, O2–Mn2–O2c; 176.84°. The Mn–N_{azide} distances are 2.205(9)–2.265(9) Å, smaller than in chain A and similar to values found in complexes reported in the literature [50–53]. The EO azide bridges show asymmetric N–N distances of 1.195(14)/1.159(13) Å and quasi-linearity expressed by N11–N12–N13 angle of 178.7(12)°. Unlike in chain A, the dihedral angle between the Mn_2N_2 planar rings (Mn2N11Mn2dN11d) is 3.69°. The closest Mn2…Mn2 distance is 3.266 Å, below the corresponding Mn1···Mn1 distance in chain A (3.618 Å) as well as 3.634(1), 3.459(3), 3.459(8), 3.455(6) and 3.472 Å in

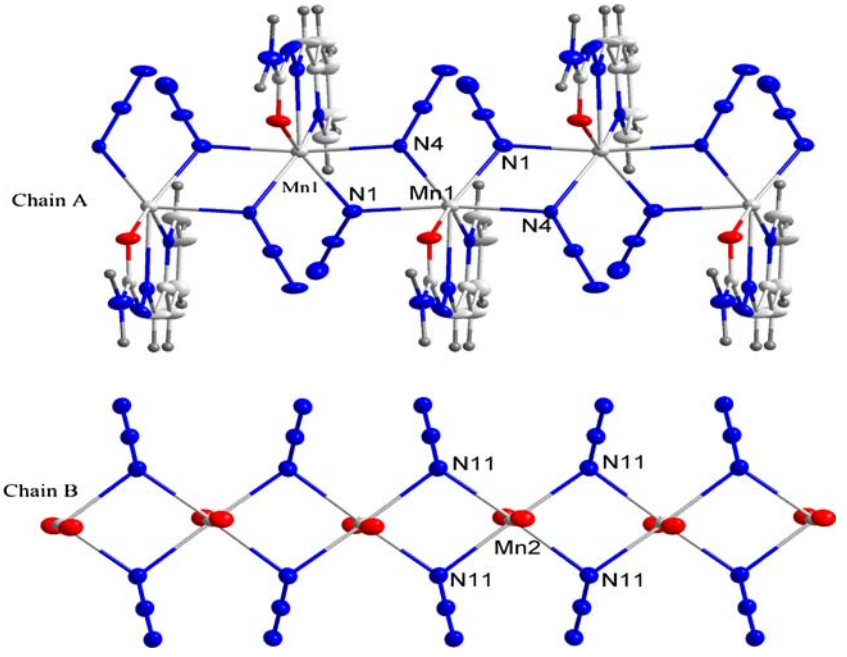

Figure 3. View of the 1D chains A and B for **1**.

similar complexes [50–53]. The bridging Mn2–N11–Mn2d angle of 93.9(4)° is smaller than found in similar complexes [50–53]. Chains A and B are connected via intermolecular hydrogen bonds into a 2-D network: (i) amino of chain A bridges two different B chains with two hydrogen bonds to azide; (ii) waters of chain B connect the chain to neighboring A chains via hydrogen bonds to carbonyl. Detailed information about hydrogen bonds is given in table 4. In the structure of **1**, distances between adjacent pyridine rings are 6.529 Å, therefore no interlayer π–π interactions are present. These distances of 6.529 Å are large compared with 3.92 Å in the structure of $[Mn(bphz)(N_3)_2]_n$ (bphz: 2-benzoylpyridine hydrazone [50]), and with distance of 3.286 Å found in $[Mn(tptz)(\mu_{1,1}\text{–}N_3)_2]_n$ (tptz: 2,4,6-tris(2-pyridyl)-1,3,5-triazine) [51].

3.3.2. $[Cd(HL)(\mu_{1,1}\text{–}N_3)_2]_n$ (2). The ORTEP diagram with atom labeling scheme of **2** is depicted in figure 4; crystal data and structure refinement of **2** are summarized in table 2. The compound crystallizes in the monoclinic system, with space group P21/c. The structure of **2** (figure 5) can be described as infinite 1-D chains of Cd bridged by double EO azides (figure 6) and extended in the direction of the crystallographic *c* axis. The Cd(II) is seven-coordinate with a distorted pentagonal–bipyramidal geometry. The equatorial plane of the pentagon is formed by two nitrogens of azide (N5 and N8) and two nitrogens and one oxygen of HL (N3, N4 and O1). Axial coordination sites are occupied by two nitrogens of two other bridging azides (N5a and N8b) with the N5aCd1N8b, 175.38(15)°. By calculating the N4N3O1N5N8Cd1 plane for the five equatorial atoms and also Cd, only Cd and N3 are approximately in this plane about 0.014 and 0.049 Å from the plane; N4 is above this plane by 0.414 Å and O1 is below by 0.360 Å with N4Cd1O1 of 129.18°, N8 and N5 are above and below by 0.583 and 0.602 Å from the plane, respectively, with

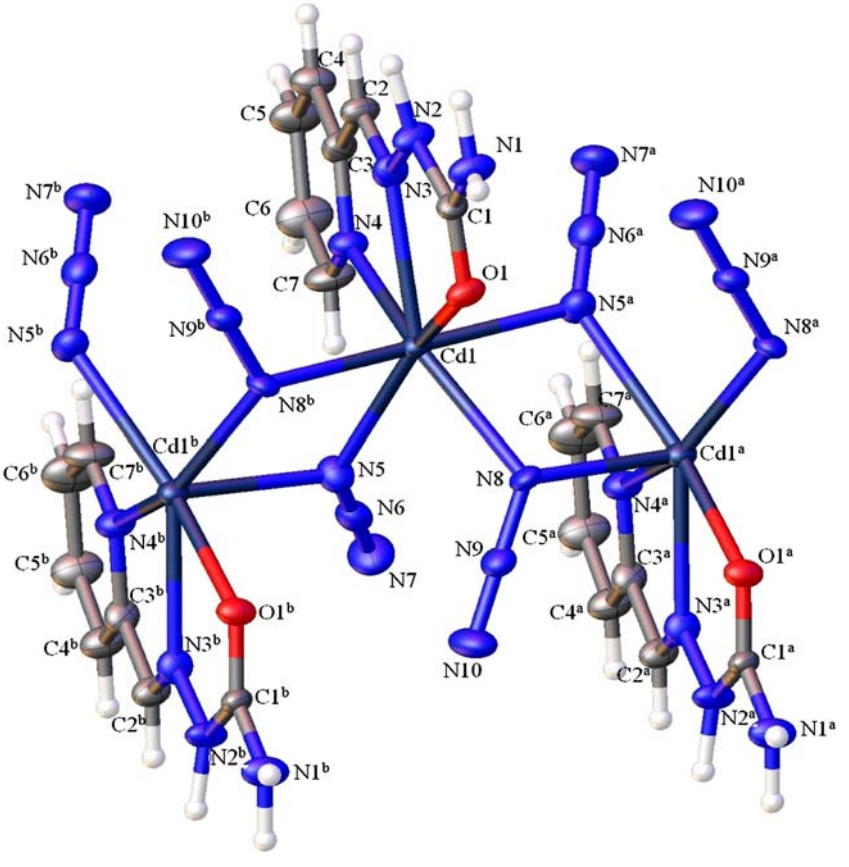

Figure 4. ORTEP diagram of **2** with symmetry equivalent atom labeling scheme.

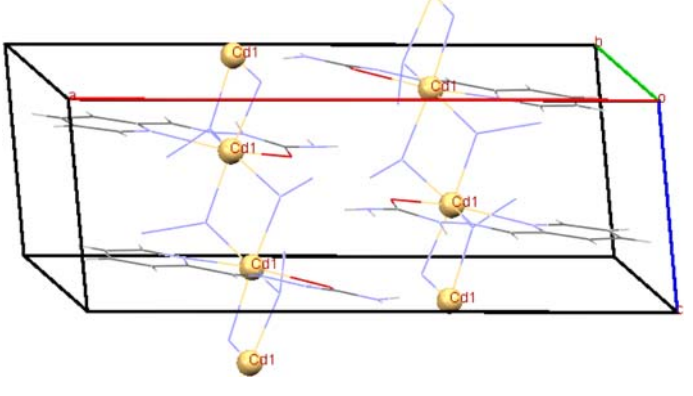

Figure 5. View of the unit cell of **2** in the direction of the crystallographic *b* axis.

N8Cd1N5 of 81.99°. The Cd–N_{azide} distances are 2.311(5)–2.443(5) Å whereas Cd–N_{HL} distances are 2.464(5) and 2.541(4) Å. The EO azide bridges are asymmetric with N–N

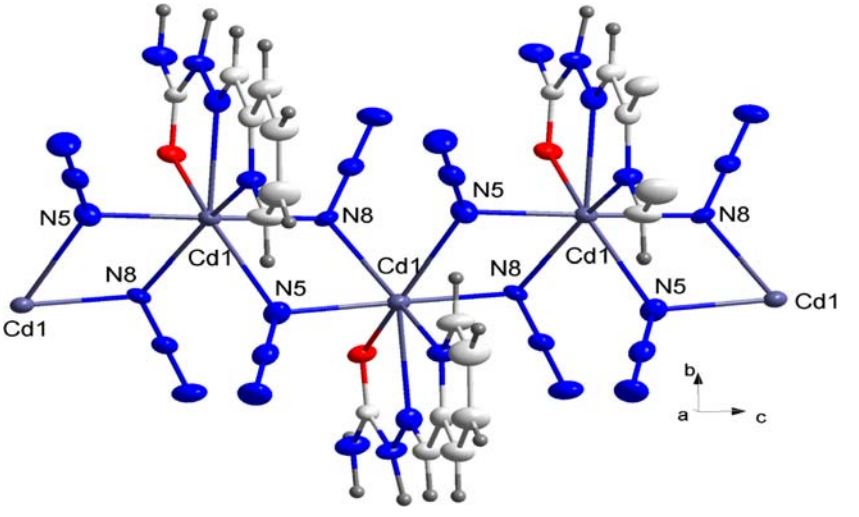

Figure 6. The view of the 1D chain of **2.**

distances of 1.200(7)/1.166(6) Å and 1.193(6)/1.156(7) Å, similar to N–N distances found in $[Cd(4\text{-}Etpy)_2(N_3)_2]_n$ (4-Etpy = 4-ethylpyridine) [54]. The azide bridges are quasi-linear, with N5–N6–N7 angles of 178.4(6)° and N8–N9–N10 of 179.4(6)°. The four-membered Cd1–N8–Cd1–N5 rings are planar but adjacent Cd1–N8–Cd1–N5 rings are mutually twisted with dihedral angle 76.60°, similar to **1**. The closest Cd1…Cd1 distance is 3.731 Å with Cd1–N5–Cd1 bridging angles of 103.10(18)° and Cd1–N8–Cd1 of 105.90(18)°. The Cd1…Cd1 distance for **2** is larger than found in corresponding compounds with the same $[Cd_2(N_3)_2]_n$ topology, 3.661(1) Å in $[Cd(4\text{-}Etpy)_2(N_3)_2]_n$ (4-Etpy = 4-ethylpyridine), 3.693(1) Å in $[Cd(3\text{-}acpy)_2(N_3)_2]_n$, 3-acpy = 3-acetyl pyridine, 3.556(2) Å in $[Cd(4\text{-}OHMepy)_2(N_3)_2]_n$ (4-OHMepy = 4-hydroxy methylpyridine) [54], 3.652(2) Å in $[Cd(2\text{-}picNO)_2(N_3)_2]_n$ (2-picNO = 2-picoline-N-oxide) [55], 3.634(2) Å in $[Cd(3\text{-}aldpy)\text{-}(H_2O)(N_3)_2]_n$ (3-aldpy = 3-pyridine carboxaldehyde) [56], and 3.561(1) Å in $[Cd(2\text{-}acpy)(N_3)_2]_n$ (2-acpy = 2-acetylpyridine) [57].

N1−H1···O1 hydrogen bonds between two amido groups and N2–H1…N10 interactions between imino group and azide, connect the chains into slabs parallel with the *bc* plane. For more information about H-bonds and bond distances see table 4. In the structure of **2**, distances between adjacent pyridyl rings in the 1-D chains are 6.549 Å, and therefore there are no interlayer π–π interactions.

3.4. *Electrochemistry*

The cyclic voltammogram of HL shows it is electroactive from 1.5 to −2 V in DMSO solvent [58,59]. There are two ligand-centered reductions at −1.1 V and −1.83 V and one oxidation at 0.90 V; all of these are attributed to pyridine ring. The cyclic voltammogram of azide displays only an irreversible oxidation at 0.85 V.

The cyclic voltammogram of **1** displays two irreversible oxidation waves at 0.87 and 0.72 V related to oxidation of HL and azide, respectively. By comparing the cyclic voltammogram of **1** with that of HL and azide, both oxidation waves in **1** are shifted to lower

potentials due to coordination. Since no waves are related to oxidation or reduction of $Mn^{2+/3+}$ centers, it is concluded that the $Mn^{2+/3+}$ centers in **1** do not contribute to its electrochemical activity. The cyclic voltammogram of **2** displays three oxidation waves at 0.78, 0.33 and −1.23 V and two reduction waves at −0.65 and −1.85 V. The oxidation waves observed at 0.78 and 0.33 V are related to oxidation of HL and azide, respectively. The oxidation wave at −1.23 V is due to oxidation Cd(0) → Cd(II) and correspondingly, there is also a reduction wave at −0.65 V caused by reduction Cd(II) → Cd(0). The reduction wave observed at −1.85 V is related to reduction of HL.

3.5. *Magnetic properties*

Variable temperature magnetic susceptibility measurements for **1** from 2 to 300 K as plots of χ_M and $1/\chi_M$ versus T are shown in figures 7 and 8, respectively, where χ_M is the molar magnetic susceptibility of one mole of Mn ions.

On decreasing from 300 K, the value of χ_M increases continuously to maximum around 4.5 K; further cooling leads to rapid decrease of susceptibility. The maximum of χ_M is related to magnetic coupling of the Mn centers. Diamagnetic contribution was estimated by using Pascal's constants $\chi_{dia} = -2.204 \cdot 10^{-4}$ cm^3/mol and subtracted from the total susceptibility. Analysis of high-temperature susceptibility [60] performed with a Curie-Weiss law (figure 7) yields Curie temperature $\theta = 11.27 \pm 0.03$ K. The positive value of θ indicates ferromagnetic exchange interactions between Mn ions [61], also demonstrated by a maximum observed at 4.5 K (see figure 7).

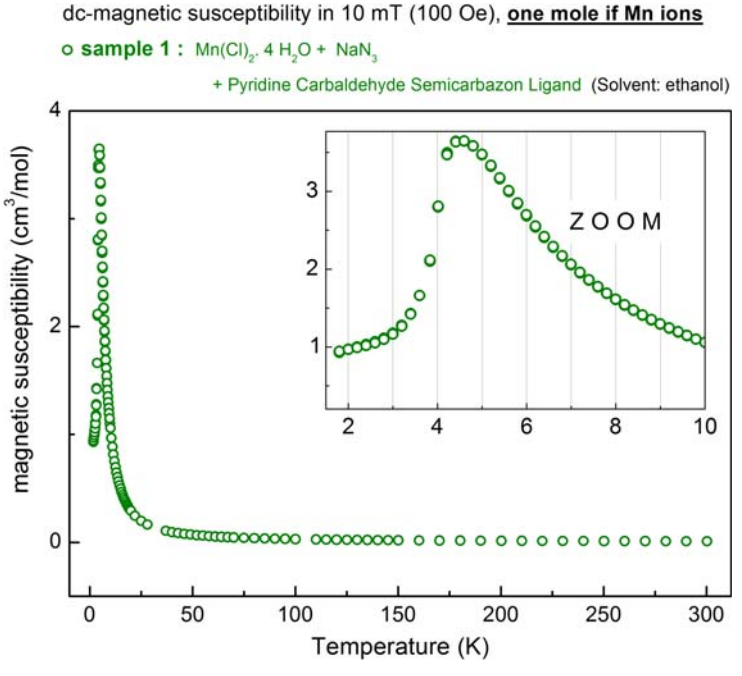

Figure 7. Variable temperature magnetic susceptibility for **1** versus T from 2 to 300K.

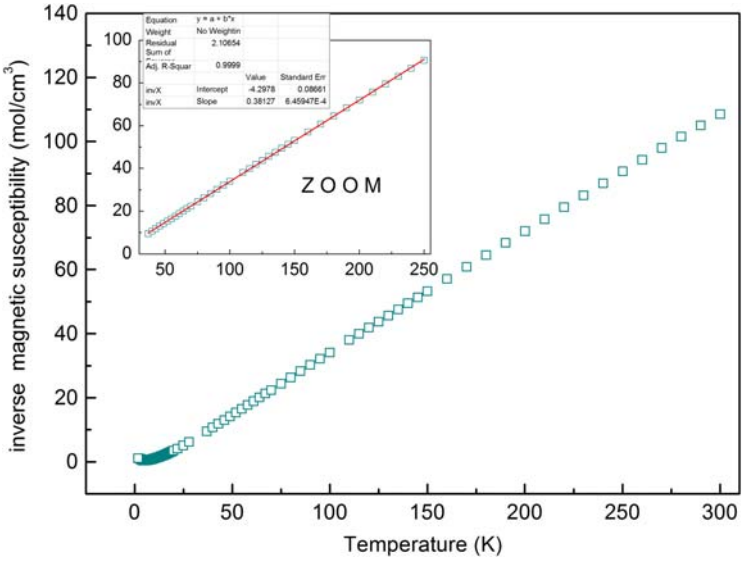

Figure 8. Variable temperature inverse magnetic susceptibility for **1** versus T from 2 to 300K.

From $\chi(T)$ (at room temperature), the effective magnetic moment may be quantified as $\mu_B = 4.69$, which is very close to that expected for spin $S = 2$ corresponding to Mn^{3+} [60]. An averaged g-factor value, $g = 1.88 \pm 0.1$, is very close to the typical value for a Mn ion.

3.6. *Antimicrobial screening*

Antimicrobial screenings of HL, **1** and **2** were tested for their effect on certain bacteria and fungi (table 5). Study of MIC values reveals that HL has weak activity. However, the metal compounds show enhanced activity against bacteria and fungi than free ligand. The increased activity of the metal chelates can be explained on the basis of chelation theory [16,18,62–64]. **2** has stronger antimicrobial activity than **1**, attributed to the atomic radius and electronegativity of Cd ions. Higher electronegativity and larger atomic radius decreases the effective positive charge on the complex molecules [16,29].

Table 5. The antimicrobial activity of HL, **1** and **2** (MIC in μg/mL).

Compound	*Bacillus subtilis*	*Staphylococcus aureus*	*Escherichia coli*	*Erwinia carotovora*	*Candida kefyr*	*Candida krusei*	*Aspergillus niger*
HL	625	1250	1250	1250	625	625	1250
1	312	625	312	312	625	625	625
2	18	39	39	18	39	39	78
Gentamicin[a]	4	8	8	8	–	–	–
Amphotricin B[b]	–	–	–	–	4	4	16
DMSO	–	–	–	–	–	–	–

[a]Gentamicin is used as the standard. MIC (μg/mL) minimum inhibitory concentration, i.e. the lowest concentration to completely inhibit the bacterial growth.
[b]Amphotricin B is used as the standard. MIC (μg/mL) minimum inhibitory concentration, i.e. the lowest concentration to completely inhibit the fungal growth.

4. Conclusion

Two new coordination polymers, $[Mn(L)(\mu_{1,1}\text{–}N_3)_2]_{2n}$ $[Mn(H_2O)_2(\mu_{1,1}\text{–}N_3)_2]_n$ (**1**) and $[Cd(HL)(\mu_{1,1}\text{–}N_3)_2]_n$ (**2**), have been synthesized (HL: pyridine-2-carbaldehyde semicarbazone). Single crystal X-ray diffraction revealed that the metal centers in **1** and **2** are coordinated by NNO of HL and are connected to each other by double EO azides forming 1-D chains. The metal centers in part A of **1** and in **2** are seven-coordinate with distorted pentagonal–bipyramidal geometry; the manganese in part B of **1** is six-coordinate with distorted octahedral geometry. Electrochemical studies demonstrate that HL, **1** and **2** are electrochemically active. Magnetic properties of **1** indicate ferromagnetic coupling below 5 K with Curie temperature $\theta = 11.27 \pm 0.03$ K as expected for EO bridging azides. The antimicrobial activities show that **1** and **2** are more active than HL. **2** has strong antimicrobial activity due to the larger radius and electronegativity of Cd(II).

Supplementary material

Crystallographic data (excluding structure factors) for all the structures reported in this paper have been deposited with the Cambridge Crystallographic Data Centre as supplementary publication nos. CCDC 843846 and 843848 for **1** and **2**, respectively. Copies of these data can be obtained free of charge on application to CCDC, 12 Union Road, Cambridge CB2 2EZ, UK; Fax: +44 1223 336033, or online via www.ccdc.cam.ac.uk/data_request/cif or by emailing data_request@ccdc.cam.ac.uk.

Acknowledgements

We gratefully acknowledge the financial support of the Tabriz University Research council and are also very much obliged to Dr. Babak Mirtamizdoust and Mr. Majid Sadeghi for their assistance. We also acknowledge support of the project Praemium Academiae of the Academy of Sciences of the Czech Republic. As well, this work is supported by Slovak Grant Agency VEGA-1/0159/09 and by the ERDF EU (European Union European regional development fund) grant under contract No. ITMS26220120005.

References

[1] D. Sadhukhan, A. Ray, R.J. Butcher, C.J. Gomez Garcia, B. Dede, S. Mitra. *Inorg. Chim. Acta*, **376**, 245 (2011).
[2] A. Dehno Khalaji, M. Amirnasr, S. Triki. *Inorg. Chim. Acta*, **362**, 587 (2009).
[3] L. Jia, N. Tang, J.J. Vittal. *Inorg. Chim. Acta*, **362**, 2525 (2009).
[4] A. Ray, G. Pilet, C.J. Gomez-Garcia, S. Mitra. *Polyhedron*, **28**, 511 (2009).
[5] A. Dehno Khalaji, H. Hadadzadeh, K. Fejfarova, M. Dusek. *Polyhedron*, **29**, 807 (2010).
[6] S. Nayak, P. Gamez, B. Kozlevcar, A. Pevec, O. Roubeau, S. Dehnen, J. Reedijk. *Polyhedron*, **29**, 2291 (2010).
[7] H. Hosseini Monfared, S. Kheirabadi, N. Asghari, P. Mayer. *Polyhedron*, **30**, 1375 (2011).
[8] H. Hosseini Monfared, V. Aghapour, M. Ghorbanloo, P. Mayer. *Appl. Catal. A*, **372**, 209 (2010).
[9] O. Pouralimardan, A.-C. Chamayou, C. Janiak, H. Hosseini-Monfared. *Inorg. Chim. Acta*, **360**, 1599 (2007).
[10] S.M. Islam, A. Singha Roy, P. Mondal, M. Mubarak, S. Mondal, D. Hossain, S. Banerjee, S.C. Santra. *J. Mol. Catal. A: Chem.*, **336**, 106 (2011).
[11] G. Bhargavi, M.V. Rajasekharan, J.-P. Costes, J.-P. Tuchagues. *Polyhedron*, **28**, 1253 (2009).
[12] P. Mukherjee, O. Sengupta, M.G.B. Drew, A. Ghosh. *Inorg. Chim. Acta*, **362**, 3285 (2009).
[13] P. Gomez-Saiz, R. Gil-Garcia, M.A. Maestro, J.L. Pizarro, M.I. Arriortua, L. Lezama, T. Rojo, M. Gonzalez-Alvarez, J. Garcia-Tojal. *J. Inorg. Biochem.*, **102**, 1910 (2008).

[14] S. Basak, S. Sen, C. Marschner, J. Baumgartner, S.R. Batten, D.R. Turner, S. Mitra. *Polyhedron*, **27**, 1193 (2008).
[15] C.-G. Liu, Y.-Q. Qiu, S.-L. Sun, N. Li, G.-C. Yang, Z.-M. Su. *Chem. Phys. Lett.*, **443**, 163 (2007).
[16] N. Raman, S. Sobha, A. Thamaraichelvan. *Spectrochim. Acta, Part A*, **78**, 888 (2011).
[17] S. Banerjee, S. Mondal, W. Chakraborty, S. Sen, R. Gachhui, R.J. Butcher, A.M.Z. Slawin, C. Mandal, S. Mitra. *Polyhedron*, **28**, 2785 (2009).
[18] G.G. Mohamed, M.A. Zayed, S.M. Abdallah. *J. Mol. Struct.*, **979**, 62 (2010).
[19] G.G. Mohamed, M.M. Omar, A.A. Ibrahim. *Spectrochim. Acta, Part A*, **75**, 678 (2010).
[20] C.M. da Silva, D.L. da Silva, L.V. Modolo, R.B. Alves, M.A. de Resende, C.V.B. Martins, A. de Fatima. *J. Adv. Res.*, **2**, 1 (2010).
[21] C. Maxim, T.D. Pasatoiu, V. Kravtsov, S. Shova, C.A. Muryn, R.E.P. Winpenny, F. Tuna, M. Andruh. *Inorg. Chim. Acta*, **361**, 3903 (2008).
[22] S. Nigam, M.M. Patel, A. Ray. *J. Phys. Chem. Solids*, **61**, 1389 (2000).
[23] N.C. Kasuga, K. Sekino, M. Ishikawa, A. Honda, M. Yokoyama, S. Nakano, N. Shimada, C. Koumo, K. Nomiya. *J. Inorg. Biochem.*, **96**, 298 (2003).
[24] N.C. Kasuga, K. Sekino, C. Koumo, N. Shimada, M. Ishikawa, K. Nomiya. *J. Inorg. Biochem.*, **84**, 55 (2001).
[25] N.C. Kasuga, K. Onodera, S. Nakano, K. Hayashi, K. Nomiya. *J. Inorg. Biochem.*, **100**, 1176 (2004).
[26] S. Chandra, A. Kumar. *Spectrochim. Acta, Part A*, **66**, 1347 (2007).
[27] C. Adhikary, D. Mal, K.-I. Okamoto, S. Chaudhuri, S. Koner. *Polyhedron*, **25**, 2191 (2006).
[28] B.-L. Liu, H.-P. Xiao, E.N. Nfor, Y. Song, X.-Z. You. *Inorg. Chem. Commun.*, **12**, 8 (2009).
[29] A.M. Madalan, M. Noltemeyer, M. Neculai, H.W. Roesky, M. Schmidtmann, A. Muller, Y. Journaux, M. Andruh. *Inorg. Chim. Acta*, **359**, 459 (2006).
[30] G.A. van Albada, M.G. van der Horst, L. Mutikainen, U. Turpeinen, J. Reedijk. *Inorg. Chim. Acta*, **367**, 15 (2011).
[31] Z. Mahendrasinh, S. Ankita, S.B. Kumar, A. Escuer, E. Suresh. *Inorg. Chim. Acta*, **375**, 333 (2011).
[32] I. Banerjee, J. Marek, R. Herchel, M. Ali. *Polyhedron*, **29**, 1201 (2010).
[33] S. Shit, P. Talukder, J. Chakraborty, G. Pilet, M.S. El Fallah, J. Ribas, S. Mitra. *Polyhedron*, **26**, 1357 (2007).
[34] W.-W. Sun, X.-B. Qian, C.-Y. Tian, E.-Q. Gao. *Inorg. Chim. Acta*, **362**, 2744 (2009).
[35] X.-T. Liu, Q.-L. Liu. *J. Mol. Struct.*, **889**, 160 (2008).
[36] E.G. Novikov, A.G. Pozdeeva, L.D. Stonov, L.A. Bakumenko. *Khim. V Sel'sk. Khoz.*, **4**, 435 (1966).
[37] E.R. Garbelini, M. Hörner, M.B. Behm, D.J. Evans, F.S. Nunes. *Z. Anorg. Allg. Chem.*, **634**, 1801 (2008).
[38] S. Chandra, S. Raizada, R. Verma. *J. Chem. Pharm. Res.*, **4**, 1612 (2012).
[39] A. Ray, S. Banerjee, R.J. Butcher, C. Desplanches, S. Mitra. *Polyhedron*, **27**, 2409 (2008).
[40] J.M. Harrowfield, H. Miyamae, B.W. Skelton, A.A. Soudi, A.H. White. *Aust. J. Chem.*, **49**, 1029 (1996).
[41] F. Marandi, B. Mirtamizdoust, A.A. Soudi, H.-K. Fun. *Inorg. Chem. Commun.*, **10**, 174 (2007).
[42] G. Mahmoudi, A. Morsali. *Inorg. Chim. Acta*, **362**, 3238 (2009).
[43] G. Mahmoudi, A. Morsali, M. Zeller. *Inorg. Chim. Acta*, **362**, 217 (2009).
[44] G. Mahmoudi, A. Morsali, M. Zeller. *Solid State Sci.*, **10**, 283 (2008).
[45] Agilent Technologies, CrysAlis PRO, Yarnton, Oxfordshire (2010).
[46] T.A. Reena, E.B. Seena, M.R. Prathapachandra Kurup. *Polyhedron*, **27**, 1825 (2008).
[47] P.F. Rapheal, E. Manoj, M.R. Prathapachandra Kurup. *Polyhedron*, **26**, 5088 (2007).
[48] V.A. Sawant, B.A. Yamar, S.K. Sawant, S.S. Chavan. *Spectrochim. Acta, Part A*, **74**, 1100 (2009).
[49] S. Banerjee, A. Ray, S. Sen, S. Mitra, D.L. Hughes, R.J. Butcher, S.R. Batten, D.R. Turner. *Inorg. Chim. Acta*, **361**, 2692 (2008).
[50] E.-Q. Gao, Y.-F. Yue, S.-Q. Bai, Z. He, S.-W. Zhang, C.-H. Yan. *Chem. Mater.*, **16**, 1590 (2004).
[51] A. Das, G.M. Rosair, M.S. El Fallah, J. Ribas, S. Mitra. *Inorg. Chem.*, **45**, 3301 (2006).
[52] R. Cortés, M. Drillon, X. Solans, L. Lezama, T. Rojo. *Inorg. Chem.*, **36**, 677 (1997).
[53] H.-Y. Wu, H.-Q. An, B.-L. Zhu, S.-R. Wang, S.-M. Zhang, S.-H. Wu, W.-P. Huang. *Inorg. Chem. Commun.*, **10**, 1132 (2007).
[54] M.A.S. Goher, F.A. Mautner, K. Gatterer, M.A.M. Abu-Youssef, A.M.A. Badr, B. Sodin, C. Gspan. *J. Mol. Struct.*, **876**, 199 (2008).
[55] F.A. Mautner, C. Gspan, M.A.S. Goher, M.A.M. Abu-Youssef. *Monatsh. Chem.*, **136**, 107 (2005).
[56] M.A.S. Goher, F.A. Mautner, M.A.M. Abu-Youssef, A.K. Hafez, A.M.A. Badr, C. Gspan. *Polyhedron*, **22**, 3137 (2003).
[57] M.A.S. Goher, F.A. Mautner, M.A.M. Abu-Youssef, A.K. Hafez, A.M.A. Badr. *J. Chem. Soc., Dalton Trans.*, 3309 (2002).
[58] S. Meghdadi, M. Amirnasr, K. Mereiter, H. Molaee, A. Amiri. *Polyhedron*, **30**, 1651 (2011).
[59] E. Tas, A. Kilic, M. Durgun, I. Yilmaz, S. Arslan. *Spectrochim. Acta, Part A*, **75**, 811 (2010).
[60] R.J. Carlin, A.J. van Duyeneveldt, Magnetic Properties of Transition Metal Compounds, Springer Verlag (1977).

[61] G. Chastanet, B. Le Guennic, C. Aronica, G. Pilet, D. Luneau, M.-L. Bonnet, V. Robert. *Inorg. Chim. Acta*, **361**, 3847 (2008).
[62] N.P. Priya. *Int. J. Appl. Biol. Pharm. Tech.*, 2 (2011).
[63] A.A. Nejo, G.A. Kolawole, A.O. Nejo. *J. Coord. Chem.*, **63**, 4398 (2010).
[64] L. Mishra, V.K. Singh. *Indian J. Chem.*, **32A**, 446 (1993).